

# Axon diameter distribution influences diffusion-derived axonal density estimation in the human spinal cord: *in silico* and *in vivo* evidence

Francesco Grussu<sup>1</sup>, Torben Schneider<sup>1,2</sup>, Ferran Prados<sup>1,3</sup>, Carmen Tur<sup>1</sup>, Sébastien Ourselin<sup>3</sup>, Hui Zhang<sup>4</sup>, Daniel C. Alexander<sup>4</sup>, and Claudia Angela Michela Gandini Wheeler-Kingshott<sup>1,5</sup>

<sup>1</sup>*NMR Research Unit, Queen Square MS Centre, Department of Neuroinflammation, UCL Institute of Neurology, University College London, London, United Kingdom*

<sup>2</sup>*Philips Healthcare, Guildford, Surrey, England*

<sup>3</sup>*Translational Imaging Group, Department of Medical Physics and Biomedical Engineering, University College London, London, United Kingdom*

<sup>4</sup>*Department of Computer Science and Centre for Medical Image Computing, University College London, London, United Kingdom*

<sup>5</sup>*Brain Connectivity Centre, C. Mondino National Neurological Institute, Pavia, Italy*

## Synopsis

Diffusion MRI-derived neurite density is a potential biomarker in neurological conditions. In the brain, neurites are commonly modelled as *sticks* for sufficiently long diffusion times and gradient durations. However, in the spinal cord, large axons are present and typical diffusion times (20-30 ms) may not be sufficiently long to support this model. We investigate via simulations and *in vivo* whether neurite density estimation is affected by the diffusion time in the spinal cord. Short diffusion times lead to bias, while long diffusion times improve accuracy but reduce precision. Therefore, a trade-off accuracy-precision needs to be evaluated depending on the application.

## Purpose

Several diffusion-weighted (DW) MRI methods provide estimates of the density of neurites, i.e. axons in white matter (WM) and dendrites in grey matter (GM), modelling them as *sticks*<sup>1,2</sup> (zero-radius cylinders). This simplification is reasonable in the long diffusion time limit<sup>3</sup> and long gradient pulse duration<sup>4</sup>, a condition practically achievable in most brain WM. However, in spinal cord WM, myelinated axons can have diameters<sup>5</sup> as large as 10-15  $\mu\text{m}$ , and the diffusion times employed to minimise the echo time  $T_E$  of DW spin echo acquisitions may not be sufficiently long to support the *stick* model. Here, we investigated whether in clinical settings sub-optimal diffusion times can affect neurite density (ND) estimation in the spinal cord, assessing diffusion time dependency of ND *in vivo* and corroborating results with simulations.

## Methods

**Simulated signal synthesis** The Camino Monte Carlo (MC) simulator<sup>6</sup> was used to synthesise DW signals from two substrates describing WM characterised by big and small axons (figure 1: *BigAxons/SmallAxons*, representative of spinal cord<sup>5</sup> and corpus callosum<sup>7</sup>), made of cylinders with gamma-distributed radii (cylinder volume fraction (CVF) of 0.65, diffusivity inside/outside 1.70  $\mu\text{m}^2/\text{ms}$ ). Four clinically feasible two-shell protocols ( $b=711$  s/mm<sup>2</sup> and  $b=2855$  s/mm<sup>2</sup>; 30 and 60 directions; gradient duration  $\delta=18$  ms) were synthesised, each characterised by a diffusion time  $T_d = \Delta - \delta/3$  among {24, 41.3, 58.7, 76} ms (gradient separation  $\Delta$  was varied).

**Simulated signal analysis** CVF was estimated with NODDI<sup>2</sup> on: i) 1000 unique sub-protocols of 25 and 50 directions at  $b=711$  s/mm<sup>2</sup> and  $b=2855$  s/mm<sup>2</sup> for infinite signal-to-noise ratio (SNR); ii) 1000 protocols with unique realisations of Rician noise (SNR of 13, 10.25, 8.09, 6.38 for increasing  $T_d$  to model the effect of longer  $T_E$ , assuming  $T_2=72$  ms and SNR=13 at  $T_d=24$  ms). Signals from substrates *BigAxons/SmallAxons* were averaged to simulate a mixture of their radius distributions.

**In vivo acquisition** Three subjects (all aged 27) were scanned axially on a 3T Philips Achieva system (cardiac gated ZOOM-EPI sequence<sup>8</sup>, cervical level C1-C3, resolution  $1 \times 1 \times 5 \text{mm}^3$ , field-of-view  $64 \times 48 \times 60 \text{mm}^3$ ,  $T_R$  12RR repeats). Three two-shell protocols ( $b=711$  s/mm<sup>2</sup> and  $b=2855$  s/mm<sup>2</sup>; 20 and 40 directions;  $\delta=22$  ms) were acquired with  $T_d \in \{21.17, 44.67, 68.67\}$  ms, varying  $\Delta$ . Subjects were scanned twice, with minimum  $T_E$  for each  $T_d$  in the first session ( $T_E \in \{67, 87.20, 111\}$  ms) and fixing  $T_E=111$  ms in the second session, to control for the different  $T_2$ -weighting and SNR implied by a variable  $T_E$ .

In vivo analysis ND was estimated fitting NODDI after slice-wise motion correction and spinal cord segmentation. We created an average DW image with good GM/WM contrast<sup>9</sup>, where we segmented GM manually and determined WM as the portion of the cord not containing GM. ND was characterised in WM calculating median and interquartile range.

## Results

Simulations Figure 2 shows the estimated CVF. At infinite SNR, CVF is underestimated for the *BigAxons* and mixture *BigAxons/SmallAxons* substrates, and increasing  $T_d$  decreases this bias. CVF shows neither bias nor  $T_d$ -dependency for the *SmallAxons* substrate. Adding noise provides similar trends, but decreases precision.

In vivo ND maps for one slice per volunteer are shown in figures 3 and 4 for the two MRI sessions. In both sessions, ND increases as  $T_d$  increases, especially in certain areas as those illustrated. Table 1 reports descriptive statistics of ND in WM and the percentage relative increase of the median ND with respect to the median at  $T_d=21.17$  ms. A trend of higher ND for longer  $T_d$  is measured in all subjects and sessions (increase of about 10%).

## Discussion and conclusion

Here we investigated whether in clinical scenarios sub-optimal diffusion times affect ND estimation in the spinal cord.

MC simulations run with a relatively long gradient pulse duration demonstrated that ND can be underestimated in microstructural geometries plausible in the spinal cord, if inadequately short diffusion times are employed. The underestimation is stronger at shorter diffusion time, but also occurs at longer diffusion time, because of the finite diameter of axons. *In vivo* experiments showed a trend of increasing ND in spinal cord WM as the diffusion time increased, not confounded by changes of echo time. This suggests that at the shortest diffusion time we probed, the assumptions of the *stick* model were not fully met in areas with large axons.

We conclude that careful design of the diffusion time is required for the estimation of ND in the spinal cord. Short diffusion times lead to biased estimates, whereas long diffusion times lead to more accurate but less precise values. A compromise between accuracy and precision needs to be evaluated according to the application.

## Acknowledgements

UCL Grand Challenges Studentships scheme. The UK MS Society and the UCL-UCLH Biomedical Research Centre for ongoing support. Project grants EPSRC EP/I027084/1 and ISRT IMG006; EPSRC EP/L022680/1, G007748 and I027084; EPSRC EP/H046410/1, EP/J020990/1 and EP/K005278; MRC MR/J01107X/1. NIHR BRC UCLH/UCL High Impact Initiative. Post-doctoral research ECTRIMS Fellowships scheme. The help of the volunteers.

## References

- [1] Behrens T. et al. Characterization and propagation of uncertainty in diffusion-weighted MR imaging. *Magnetic Resonance in Medicine* 2003; 50(5): 1077-1088.
- [2] Zhang H. et al. NODDI: practical in vivo neurite orientation dispersion and density imaging of the human brain. *NeuroImage* 2012; 61(4): 1000-1016.
- [3] Sen P. Time-dependent diffusion coefficient as a probe of geometry. *Concepts in Magnetic Resonance Part A* 2004; 23A(1): 1-21.
- [4] Mitra P. and Halperin B. Effects of finite gradient-pulse widths in pulsed-field-gradient diffusion measurements. *Journal of Magnetic Resonance Series A* 1995; 113(1): 94-101.

[5] Makino M. et al. Morphometric study of myelinated fibers in human cervical spinal cord white matter. *Spine* 1996; 21: 1010-1016.

[6] Hall M. and Alexander D. Convergence and parameter choice for Monte-Carlo simulations of diffusion MRI. *IEEE Transactions on Medical Imaging* 2009; 28(9): 1354-1364.

[7] Alexander D. et al. Orientationally invariant indices of axon diameter and density from diffusion MRI. *NeuroImage* 2010; 52(4): 1374-1389.

[8] Wheeler-Kingshott C. et al. ADC mapping of the human optic nerve: increased resolution, coverage, and reliability with CSF-suppressed ZOOM-EPI. *Magnetic Resonance in Medicine* 2002; 47(1): 24-31.

[9] Kearney H. et al. Spinal cord grey matter abnormalities are associated with secondary progression and physical disability in multiple sclerosis. *Journal of Neurology, Neurosurgery and Psychiatry*, 2015; 86(6): 608-614.

Figures

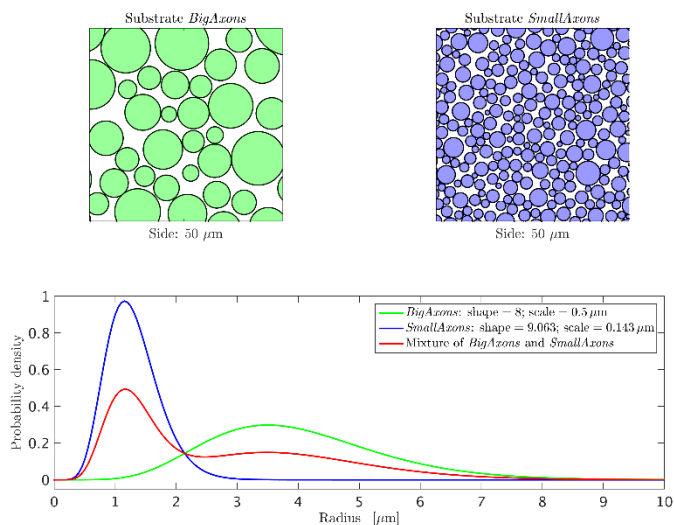


Figure 1: substrates employed for MC simulations. Top: detail of 50 μm x 50 μm of substrate *BigAxons* (to the left, with axons in green) and *SmallAxons* (to the right, with axons in blue). Bottom: radius distribution of substrates *BigAxons* (green), *SmallAxons* (blue) and a mixture of the two (red). For all substrates, the cylinder volume fraction (CVF) was set to 0.65. In substrates *BigAxons* and *SmallAxons*, radii follow a gamma distribution controlled by a scale and a shape parameter.

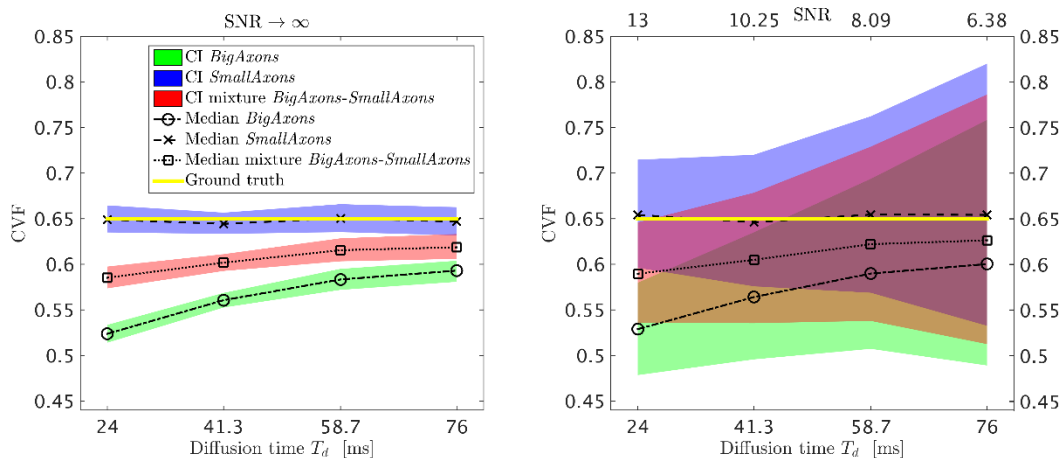


Figure 2: cylinder volume fraction (CVF) estimated with NODDI from synthetic signals. To the left, results from fitting performed at infinite SNR. To the right, results from fitting with SNR at  $b=0$  decreasing with increasing diffusion time, to account for the longer echo time required. Medians and 95% confidence interval (CI) over the 1000 repetitions of the fitting are reported for all simulated substrates. Ground truth CVF is also shown, in yellow.

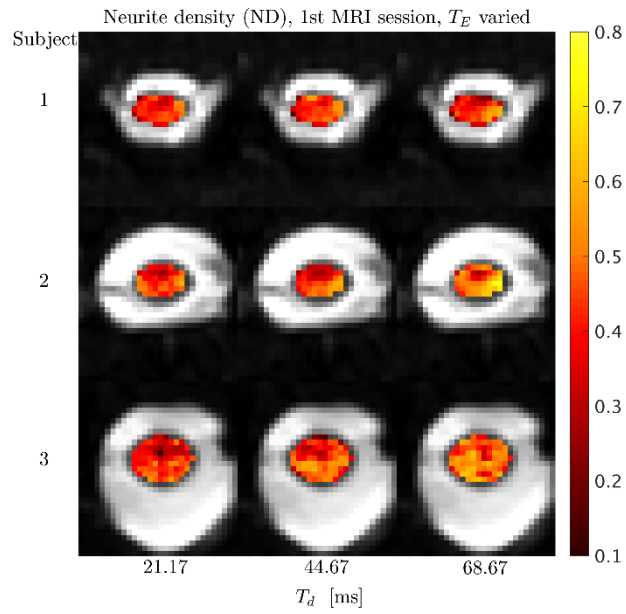


Figure 3: examples of neurite density (ND) maps from the first scanning session (the minimum echo time achievable for each diffusion time was used), overlaid onto the mean  $b=0$  image. Different subjects are illustrated along different rows, whereas maps corresponding to different diffusion times are illustrated along different columns.

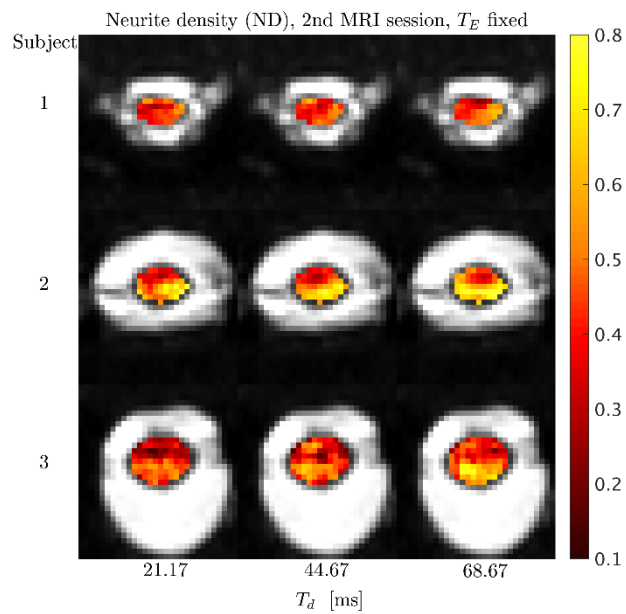


Figure 4: examples of neurite density (ND) maps from the second scanning session (echo time fixed to 111 ms for all diffusion times), overlaid onto the mean  $b=0$  image. Different subjects are illustrated along different rows, whereas maps corresponding to different diffusion times are illustrated along different columns. The same MRI slices shown in figure 3 are reported.

Subject	$T_d$ [ms]	1st MRI session		2nd MRI session	
		ND in WM	% increase	ND in WM	% increase
1	21.17	0.44 (0.38; 0.50)	-	0.44 (0.39; 0.53)	-
1	44.67	0.48 (0.42; 0.56)	10.6 %	0.50 (0.43; 0.58)	13.3 %
1	68.67	0.47 (0.37; 0.54)	6.8 %	0.49 (0.42; 0.59)	12.7 %
2	21.17	0.42 (0.36; 0.49)	-	0.44 (0.36; 0.51)	-
2	44.67	0.45 (0.39; 0.53)	6.7 %	0.45 (0.37; 0.54)	2.5 %
2	68.67	0.46 (0.40; 0.54)	9.4 %	0.48 (0.40; 0.60)	10.8 %
3	21.17	0.42 (0.37; 0.49)	-	0.40 (0.33; 0.49)	-
3	44.67	0.45 (0.39; 0.52)	6.7 %	0.41 (0.32; 0.50)	1.9 %
3	68.67	0.47 (0.38; 0.56)	11.1 %	0.46 (0.37; 0.55)	14.8 %

Table 1: medians and interquartile range of neurite density (ND) distributions in subjects' white matter (WM). Values from both MRI sessions are reported (1st session: echo time increasing for increasing diffusion time; second session: echo time fixed to 111 ms for all diffusion times). The percentage increase of the median ND with respect to the median ND at the shortest diffusion time (21.17 ms) is also reported for reference.